THE JOURNAL OF BIOLOGICAL CHEMISTRY VOL. 285, NO. 10, pp. 7165–7175, March 5, 2010

Disruption of the K^+ Channel β-Subunit KCNE3 Reveals an Important Role in Intestinal and Tracheal Cl^- Transport*[S]

Received for publication, July 22, 2009, and in revised form, December 9, 2009 Published, JBC Papers in Press, January 5, 2010, DOI 10.1074/jbc.M109.047829

Patricia Preston[‡], Lena Wartosch[‡], Dorothee Günzel[§], Michael Fromm[§], Patthara Kongsuphol[¶], Jiraporn Ousingsawat[¶], Karl Kunzelmann[§], Jacques Barhanin[‖], Richard Warth[¶], and Thomas J. Jentsch[‡1]

From the [‡]Leibniz-Institut für Molekulare Pharmakologie (FMP) and Max-Delbrück-Centrum für Molekulare Medizin (MDC), 13125 Berlin, Germany, the [§]Institut für Klinische Physiologie, Charité Universitätsmedizin Berlin, 12203 Berlin, Germany, the [¶]Institut für Physiologie, Universität Regensburg, 93053 Regensburg, Germany, and the [‖]Transport Ionique Aspects Normaux et Pathologiques, CNRS and Université Nice Sophia-Antipolis, 06108 Nice Cedex 2, France

The KCNE3 β-subunit constitutively opens outwardly rectifying KCNQ1 (Kv7.1) K^+ channels by abolishing their voltage-dependent gating. The resulting KCNQ1/KCNE3 heteromers display enhanced sensitivity to K^+ channel inhibitors like chromanol 293B. KCNE3 was also suggested to modify biophysical properties of several other K^+ channels, and a mutation in *KCNE3* was proposed to underlie forms of human periodic paralysis. To investigate physiological roles of KCNE3, we now disrupted its gene in mice. *kcne3*$^{-/-}$ mice were viable and fertile and displayed neither periodic paralysis nor other obvious skeletal muscle abnormalities. KCNQ1/KCNE3 heteromers are present in basolateral membranes of intestinal and tracheal epithelial cells where they might facilitate transepithelial Cl^- secretion through basolateral recycling of K^+ ions and by increasing the electrochemical driving force for apical Cl^- exit. Indeed, cAMP-stimulated electrogenic Cl^- secretion across tracheal and intestinal epithelia was drastically reduced in *kcne3*$^{-/-}$ mice. Because the abundance and subcellular localization of KCNQ1 was unchanged in *kcne3*$^{-/-}$ mice, the modification of biophysical properties of KCNQ1 by KCNE3 is essential for its role in intestinal and tracheal transport. Further, these results suggest *KCNE3* as a potential modifier gene in cystic fibrosis.

Voltage-gated K^+ channels are tetramers of identical or homologous subunits that form a single, common ion-selective pore. In many K^+ channels these complexes of pore-forming α-subunits associate with ancillary β-subunits that may be cytosolic (1) or may span the lipid bilayer with one (2) or several (3) transmembrane domains. These β-subunits may influence the subcellular trafficking of K^+ channels or change their regulation and biophysical properties. The *KCNE* gene family of β-subunits, which was identified by expression cloning in *Xenopus* oocytes (2), encodes five different proteins (KCNE1–5) that display a single transmembrane-spanning domain and an extracellular N terminus (for reviews see Refs. 4 and 5). Despite minK (minimal K channel, an old name for KCNE1) being a misnomer, KCNE2-KCNE5 are sometimes called MirP1–4 for MinK-related peptide (5, 6).

In heterologous expression, KCNE proteins influence the properties of an astoundingly large number of different K^+ channels (5). It is questionable whether all of these promiscuous interactions are of biological significance *in vivo*. The relevance of just a few of these interactions has been established beyond reasonable doubt. KCNQ1/KCNE1 heteromers mediate the slowly activating I_{Ks} current of the myocardium and are involved in inner ear K^+ secretion, as became evident from *KCNE1* mutations in human cardiac arrhythmia and deafness (7–9) and from *kcne1* knock-out (KO)[2] mice (10, 11). The situation is less clear for KCNE2, which may modulate HERG (6), KCNQ1 (12), KCNQ2/3 (13), and Kv4 (14) K^+ channels. Variants in the *KCNE2* gene may cause human cardiac arrhythmia by altering HERG currents (6), but *kcne2*$^{-/-}$ mice rather showed reduced cardiac Kv1.5 and Kv4.2 currents (15). KCNQ1/KCNE2 heteromers are important for gastric acid secretion as revealed by *kcnq1*$^{-/-}$ (16–18) and *kcne2*$^{-/-}$ mice (19).

Whereas KCNE1 significantly slows and enhances the depolarization-induced activation of KCNQ1 currents (20, 21), KCNE3 abolishes its voltage dependence. KCNQ1/KCNE3 heteromers yield instantaneous, nearly ohmic whole cell currents (22). Similar effects on gating were observed with KCNQ1/KCNE2 co-expression, although current amplitudes were much smaller (12, 23). Either β-subunit affects the movement of the voltage-sensing S4 domain of KCNQ1 (24). KCNQ1/KCNE3 currents could be stimulated by cAMP (22) and showed increased sensitivity to the inhibitors chromanol 293B and clotrimazole (22), as well as to XE991 (25). KCNE3 did not affect KCNQ2/3 but suppressed KCNQ4 and HERG currents (22). KCNE3 was also reported to interact with Kv2.1, Kv3.1, and Kv3.2 K^+ channels (26, 27) in brain and with Kv3.4 in skeletal muscle (28). *In situ* hybridization (22) and immunofluorescence (29) revealed co-expression of KCNQ1 and KCNE3 in intestinal epithelial cells. This led to the speculation that KCNQ1/KCNE3 mediates the chromanol 293B- and clotrima-

* This work was supported in part by the Prix Louis Jeantet de Médecine (to T. J. J.) and Deutsche Forschungsgemeinschaft Grant SFB699-A6 (to K. K.).
[S] The on-line version of this article (available at http://www.jbc.org) contains supplemental text, Table S1, and Figs. S1–S5.
[1] To whom correspondence should be addressed: Leibniz-Institut für Molekulare Pharmakologie and Max-Delbrück-Centrum für Molekulare Medizin, Robert-Rössle-Strasse 10, D-13125 Berlin, Germany. Tel.: 49-30-9406-2961; E-mail: Jentsch@fmp-berlin.de.

[2] The abbreviations used are: KO, knock-out; Chromanol 293B or C293B, trans-6-cyano-4-(*N*-ethylsulfonyl-*N*-methylamino)-3-hydroxy-2,2-dimethyl-chromane; CFTR, cystic fibrosis transmembrane conductance regulator; FSK, forskolin; IBMX, 3-isobutyl-1-methylxanthine; PBS, phosphate-buffered saline; WT, wild type; ENaC, epithelial sodium channel.

zole-inhibitable K^+ current of intestinal epithelia (22), which may stimulate intestinal Cl^- secretion by increasing the electrochemical driving force for apical Cl^- exit. It has remained unclear whether KCNE3 is needed to direct KCNQ1 to the basolateral membrane of epithelia. A KCNE3 sequence abnormality (R83H) reportedly underlies periodic paralysis in two families (28) and was found in a patient with thyrotoxic hypokalemic periodic paralysis (30). However, the same sequence variant was also found in control groups (31–33).

To clarify the physiological functions of KCNE3, we have now disrupted its gene in mice. We conclude that KCNE3 is important for ion transport across intestinal and tracheal epithelia but lacks an important role in skeletal muscle. Because the KCNQ1 α-subunit is neither unstable nor missorted without KCNE3, the transport properties intrinsic to homomeric KCNQ1 are incompatible with a function in transepithelial transport. Because other important biological roles of KCNQ1 in the heart, inner ear, and stomach require its association with KCNE1 or KCNE2 (7–11, 19), KCNQ1 may always need a KCNE subunit for proper physiological function.

EXPERIMENTAL PROCEDURES

Generation of kcne3 Null Mice—We targeted the *kcne3* gene by homologous recombination in R1 129/SvJ embryonic stem cells. The vector was designed to allow Cre-recombinase-mediated deletion of exon 4, which contains the entire coding region (see Fig. 1*A*; see supplemental materials for further details). Correct targeting was checked by Southern blot analysis using 3′ and 5′ probes that detect bands of 6 and 8 kb, respectively, in BglI-digested genomic DNA. Removal of exon 4 and the neomycin selection cassette was confirmed by Southern blot analysis (see Fig. 1*B*). All of the experiments described here were performed in a mixed 129/SvJ-C57BL/6 genetic background, using wild type littermates as controls.

Northern Blot Analysis—Total RNA was prepared from various mouse organs using TRIzol reagent (Invitrogen) according to the manufacturer's instructions. mRNA was purified from total RNA using Dynabeads oligo$(dT)_{25}$ (Invitrogen). For Northern blots, 1.5 μg of mRNA/lane were separated by denaturing formaldehyde agarose gel electrophoresis. The kcne3 probe (625 bp generated with primers CACATTCCAGCTCTTCCCATACC and CACATCAGATCATAGACACACGG) and the β-actin probe (459 bp generated with primers TTCTTTGCAGCTCCTTCGTTGCCG and TGGATGGCTACGTACATGGCTGGG) were amplified from mouse genomic and cDNA, respectively, and cloned into pGEM®-T Easy (Promega, Mannheim, Germany). The probes were obtained by NotI digestion and after purification were labeled with ^{32}P-dCTP (Rediprime II; Amersham Biosciences). Hybridization was carried out overnight at 42 °C in Ultrahyb buffer (Ambion, Darmstadt, Germany). Hybridization signals were detected using a Phospho-Imager Bas-1500 (Fujifilm, Düsseldorf, Germany).

KCNE3 Antibody Generation—A peptide representing the entire cytoplasmic C terminus of mouse KCNE3 (RSRKVDKRSDPYHVYIKNRVSMI) was synthesized by Dr. M. Beyermann (Leibniz-Institut für Molekulare Pharmakologie). It was coupled via maleimidobenzoic acid-*N*-hydroxysuccinimide ester to keyhole limpet hemocyanine using a cysteine residue added to its N terminus. Antisera were obtained from rabbits injected six times within 90 days (Pineda Antikörper-Service, Berlin, Germany) with the carrier-coupled peptide and were purified by affinity against the peptide. One of the purified antisera showed specificity in Western blots of transfected COS-7 cells and WT/KO membrane preparations of various tissues and recognized KCNE3 in immunofluorescence in intestinal and tracheal tissue sections. Staining was specific as revealed by the absence of signals in KO tissues.

Western Blot Analysis—COS7 cells were transfected with an expression plasmid (pcDNA3) containing the human KCNE3 cDNA downstream of an hemagglutinin tag fused in frame. After ~40 h of expression, the cells were detached mechanically in Ca^{2+}-free phosphate-buffered saline (PBS), and the cell membranes were prepared as described below. For Western blots of murine tissues, the mice were perfused transcardially with PBS to remove blood. The organs were dissected, snap-frozen in liquid N_2, minced in a mortar, transferred into ice-cold homogenization buffer (100 mM NaCl, 1 mM EDTA, 50 mM HEPES, pH 7.5, and protease inhibitors (Complete® and Pefabloc; Roche Applied Science)), and homogenized in a glass homogenizer. The membranes were pelleted from post-nuclear supernatants (~100.000 × *g* for 30 min at 4 °C) and resuspended in lysis buffer (homogenization buffer supplemented with 1% SDS). Protein concentration was measured by BCA assay kit (Uptima-Interchim, Montluçon, France). For deglycosylation, the membrane fractions were denatured for 15 min at 55 °C, diluted in deglycosylation buffer (10 mM EDTA, 0.5% Nonidet P-40, 50 mM HEPES, pH 7.4, and Complete® and Pefabloc proteinase inhibitors) and supplemented with *N*-glycosidase F (0.4 unit/25 μg of total protein; Roche Applied Science). After incubation for 1 h at 37 °C, the samples were diluted in Laemmli sample buffer and incubated for 15 min at 55 °C. The membrane preparations for the detection of KCNQ1 were not deglycosylated. For Western blots, equal amounts of proteins (~50 μg) were loaded on SDS-polyacrylamide gels (4–12% Bis-Tris gradient gels) and blotted onto a polyvinylidene difluoride membrane. The membranes were incubated with the rabbit anti-KCNE3, rabbit anti-KCNQ1 (29), mouse anti-flotillin-1 (BD Biosciences Pharmingen, San Diego, CA), or mouse α-actin antibodies (Sigma) followed by an incubation with secondary antibodies conjugated to horseradish peroxidase (Chemicon, Schwalbach, Germany) and detection by chemiluminescence (SuperSignalWest; Pierce).

Immunofluorescence—The mice were perfused transcardially with PBS followed by 4% paraformaldehyde in PBS. Paraffin-embedded sections of trachea, stomach, small intestine, and colon were incubated in Roti-histol (Carl Roth, Karlsruhe, Germany) followed by a graded alcohol series and then boiled for 10 min in a microwave oven in 10 mM citrate buffer, pH 6 (tracheal sections only 3 min). The sections were cooled down slowly, washed twice with PBS, and then incubated in PBS, 1% SDS for 15 min. The tracheal sections were incubated at room temperature with 0.05% trypsin (in 0.1% $CaCl_2$, 0.05 M Tris, pH 7.8) for 10 min. After 1 h in blocking solution (2% normal goat serum, 1% bovine serum albumin, 0.05% Tween, and 0.2% Triton X-100 in PBS), the sections were incubated with rabbit anti-KCNE3, anti-KCNQ1 (29), or mouse anti-H^+/K^+ ATPase

β-subunit (Dianova, Hamburg, Germany) primary antibodies (diluted in blocking solution) overnight at 4 °C. The sections were then incubated with goat anti-rabbit and goat anti-mouse IgG coupled to Alexa Fluor 488 and 545, respectively, and the nuclear stain Topro-3 1:5000 (Invitrogen), which under our conditions also partially stained the cytoplasm. Analysis was done by confocal microscopy (Zeiss LSM 510 META, Berlin, Germany) using sequential excitation for double-labeled preparations.

Histology—The mice were perfused transcardially as described above, and the tissues were embedded in paraffin. 6-μm sections were stained according to standard protocols.

Serum, Feces, and Urinary Analysis—Blood was drawn from the heart of WT and KO mice under isoflurane anesthesia, and the plasma samples were analyzed. The mice were kept in metabolic cages (Phymep, Paris, France) for 6 days. Weight, food, and water intake were controlled daily. Urine and feces were collected daily. The feces were dried at 95 °C for 3 h, weighed, and dissolved overnight in 0.75 M HNO_3 at room temperature. After homogenization in a glass homogenizer and centrifugation to remove insoluble material, the supernatant was analyzed by flame photometry (IL 943 Flame Photometer; Instrumentation Laboratory, Milano, Italy). The concentrations of creatinine, glucose, proteins, and electrolytes were determined by the Institut für Labormedizin (Helios Klinikum, Berlin-Buch, Germany).

Ussing Chamber Experiments for Intestine—The mice were anesthetized and killed by inhalation of 100% CO_2. Late distal colon, ileum, or jejunum was dissected, cut open along the mesenteric insertion, and partially stripped as described in Ref. 34. The tissue was mounted in a container system with an effective epithelial area of 0.05 cm^2 (see Ref. 35 for details) and placed in a Ussing chamber for small tissue samples (36). Bath solution contained 140 mM Na^+, 124 mM Cl^-, 5.4 mM K^+, 1.2 mM Ca^{2+}, 1.2 mM Mg^{2+}, 2.4 mM HPO_4^-, 0.6 mM $H_2PO_4^-$, 21 mM HCO_3^-, 10 mM D(+)-glucose, 10 mM D(+)-mannose, 2.5 mM glutamine, and 0.5 mM β-OH-butyrate. A temperature-controlled bubble lift ensured continuous chamber perfusion and equilibration of the solution with 95% O_2, 5% CO_2 to maintain pH 7.4 at 37 °C. The addition of 50 mg/liter piperacillin (Hexal AG, Holzkirchen, Germany) and 10 mg/liter zienam (MSD Sharp & Dohme GmbH, Haar, Germany) inhibited bacterial growth. Tetrodotoxin (serosal, 1 μM), indomethacin (mucosal and serosal, 2 μM) and amiloride (mucosal, 10 μM) were applied to inhibit neuronal activity, prevent prostaglandin formation, and block apical Na^+ channels, respectively. The experiments were performed under short circuit conditions using a computer-controlled voltage clamp device (CVC 6; Fiebig, Berlin, Germany). Prior to each experiment, the resistance of the bath solution between the voltage-sensing electrodes was determined and taken into account.

Ussing Chamber Experiments for Trachea—The tracheas were dissected, opened longitudinally on the opposite side of the cartilage free zone, and transferred into an ice-cold buffer solution of 145 mM NaCl, 0.4 mM KH_2PO_4, 1.6 mM K_2HPO_4, 6 mM D(+)-glucose, 1 mM $MgCl_2$, 1.3 mM calcium gluconate, pH 7.4) containing amiloride (10 μM). The tracheal samples were mounted in an Ussing chamber with a circular aperture of 0.785 mm^2. Luminal and basolateral sides of the epithelium were perfused continuously at a rate of 5 ml/min (T = 37 °C). The experiments were carried out under open circuit conditions. The data were collected continuously using PowerLab (AD-Instruments). The values for transepithelial voltages (V_{te}) were referred to the serosal side of the epithelium. The transepithelial resistance (R_{te}) was determined by applying short (1 s) current pulses (ΔI = 0.5 μA). R_{te} and equivalent short circuit currents (I_{sc}) were calculated according to Ohm's law ($R_{te} = \Delta V_{te}/\Delta I$, $I_{sc} = V_{te}/R_{te}$).

Rotarod Performance—Eight WT and eight KO animals were first kept for 15 days under the hypokalemic diet, and in the control group eight WT and eight KO animals were kept under standard diet. Animals from both groups were randomly observed several times a day, with no signs of periodic paralysis becoming apparent. On day 16, the animals were accustomed to the accelerating rotarod apparatus (TSE Systems, Inc., Chesterfield, MO) by placing them on the rod at the lowest speed (4 rpm) for 3 min. After ~5 min of rest, the mice were tested in the accelerating mode (4–40 rpm), and the time until they fell from the rod was recorded.

Data and Statistical Analysis—The results are given as the means ± S.E. The statistical significance was determined using two-tailed Student's t test with two-sample unequal variance.

RESULTS

Generation of kcne3 Knock-out Mice—The *kcne3* gene was disrupted by homologous recombination in mouse embryonic stem cells. Exon 4, which contains the entire open reading frame, was flanked with loxP sequences (Fig. 1*A*). Removal of exon 4 *in vivo* using Cre-recombinase-expressing deleter mice resulted in a constitutive deletion of *kcne3* as revealed by Southern blot analysis (Fig. 1*B*) and the absence of *kcne3* transcripts in Northern analysis (Fig. 2*A*). Western blots and immunohistochemistry of intestinal and tracheal sections confirmed the absence of the KCNE3 protein (see below). Homozygous *kcne3* KO mice (*kcne3*$^{-/-}$ mice) were viable, fertile, and did not show any obvious phenotype over their entire lifespan. Moreover, histological analysis of a number of tissues (colon, small intestine, stomach, trachea, brain, and skeletal muscle; supplemental Fig. S1), as well as lung, kidney, and heart (*data not shown*) did not reveal any morphological alteration in *kcne3*$^{-/-}$ mice. No abnormalities in electrolytes or other parameters were detected in serum and urine (supplemental Table S1).

Tissue Distribution and Subcellular Localization of KCNE3—In view of divergent reports on KCNE3 tissue distribution (22, 25, 27–29, 37), we investigated its expression pattern on both RNA and protein levels. Northern blot analysis of several mouse tissues (Fig. 2*A*) revealed prominent KCNE3 expression in the gastrointestinal tract. Relatively low *kcne3* transcript levels were found in the stomach and duodenum, and the highest levels were found in the colon (Fig. 2*A*). No signals were detected in *kcne3*$^{-/-}$ colon, proving the specificity of our probe and confirming the disruption of the *kcne3* gene. *kcne3* transcript levels were below our detection limit in brain, heart, and skeletal muscle.

A KCNE3 antibody was raised in rabbits against a peptide representing its entire cytoplasmic C terminus. In Western

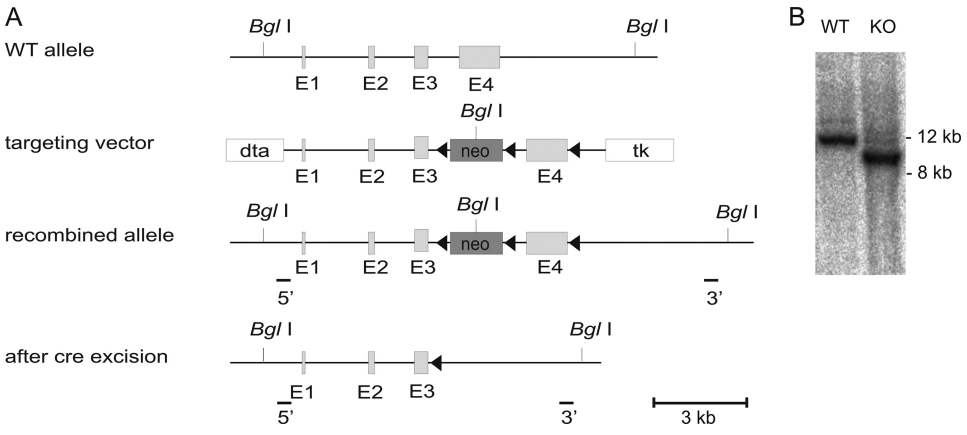

FIGURE 1. **Generation of *kcne3* KO mice.** *A*, strategy for disrupting the mouse *kcne3* gene. *Top model*, WT allele with exons depicted as boxes. Exon 4 contains the entire coding region. *Lower models*, targeting construct containing a neomycin cassette (*neo*) as positive and the diphtheria toxin A cassette (*dta*) and thymidine kinase (*tk*) as negative selection markers. The neomycin cassette was flanked by loxP sites (◀). A third loxP site was inserted after exon 4. In the recombined allele, the neomycin cassette introduced a new BglI restriction site, giving rise to ~6- and ~8-kb BglI restriction fragments. The KO allele (*bottom*) is obtained by Cre-recombinase mediated excision of exon 4. A ~9.5-kb BglI restriction fragment (that is shorter than the ~12-kb fragment of the WT allele; see *B*) may be detected with 5′ and 3′ probes (*bars* at *bottom*) by Southern blotting. *B*, Southern blot analysis of tail DNA from WT and KO mice using the 5′ probe.

blots of colon membrane preparation it specifically detected several faint bands between 20 and 30 kDa that may represent differentially glycosylated KCNE3 species (supplemental Fig. S2*B*) that were also detected by anti-hemagglutinin in transfected cells (supplemental Fig. S2*A*). Deglycosylation with peptide *N*-glycosidase F was necessary to detect a single KCNE3-specific band that was absent from KO tissues (Fig. 2*B* and supplemental Fig. S2*C*). These Western blots confirmed robust expression of KCNE3 in the intestine, in particular in colon, and revealed weaker expression in stomach and trachea. By contrast, no KCNE3 protein could be detected in brain, heart, and skeletal muscle (Fig. 2*B*).

Consistent with previous work (29, 38), both the KCNE3 β-subunit and the KCNQ1 α-subunit were detected by immunohistochemistry in basolateral membranes of intestinal epithelial cells from duodenum to colon (Fig. 3). KCNE3 staining was lost in *kcne3*$^{-/-}$ mice (Fig. 3, *B* and *F*), whereas staining for KCNQ1 remained unchanged (Fig. 3, *C*, *D*, *G*, and *H*). This observation demonstrates that neither the stability nor the subcellular localization of the KCNQ1 protein depends on its association with KCNE3. Western blot analysis confirmed that KCNQ1 levels were indistinguishable between WT and KO tissues (supplemental Fig. S3).

A previous study that used a different antibody failed to detect KCNE3 in the stomach (29). However, agreeing with our Northern and Western blot analysis (Fig. 2, *A* and *B*), KO-controlled staining revealed that KCNE3 was present in basolateral membranes of epithelial cells at the bottom of gastric glands (Fig. 4, *A*, *C*, and *D*–*F*). KCNQ1 antibodies yielded a similar basolateral staining pattern at these positions and additionally strongly labeled other cells located closer to the opening of the gland in a diffuse cytoplasmic pattern (Fig. 4, *H* and *I*). As described previously (17, 29), KCNQ1 co-localized in these latter cells with the H^+,K^+-ATPase (Fig. 4*I*), identifying them as parietal cells. These acid-secreting cells are known to express KCNE2 (18, 29). By contrast, cells stained for KCNE3 were not positive for the H^+,K^+-ATPase (Fig. 4, *A*–*D*). We conclude that KCNE2 and KCNE3 may assemble with KCNQ1 in distinct cells types, KCNQ1/KCNE2 being in apical and tubulovesicular membranes of acid-secreting parietal cells, whereas KCNQ1/KCNE3 is present in basolateral membranes of chief (or zymogenic) cells. No changes in gastric morphology were observed in *kcne3*$^{-/-}$ mice (supplemental Fig. S1, *A* and *B*), quite in contrast to the disruption of *kcne2*, which led to gastric glandular hyperplasia (19) and impaired acid secretion that depends on KCNQ1/KCNE2 channels in parietal cells (18, 29).

We next studied the trachea where we had detected KCNE3 expression at the protein level (Fig. 2). The KCNE3 antibody stained basolateral membranes of surface epithelia cells in a beaded pattern (Fig. 5), resembling the signal obtained with a KCNQ1 antibody in that tissue (39). The staining for KCNE3 was specific because it was absent from *kcne3*$^{-/-}$ trachea (Fig. 5*B*). Not all cells appeared positive for KCNE3.

KCNQ1/KCNE3 K^+ Channels in Intestinal Chloride Secretion—Based on studies using inhibitors such as chromanol 293B, K^+ channels containing the KCNQ1 α-subunit have been suggested to be crucial for colonic chloride secretion (40–44). The physiological importance of colonic chloride secretion is evident from the meconium ileus observed upon mutations in the CFTR Cl^- channel gene (45) and from the massive Cl^- diarrhea observed in cholera. Basolateral K^+ channels are thought to increase the driving force for apical Cl^- exit by hyperpolarizing the basolateral membrane and, as a consequence, also the apical membrane of colonic epithelial cells (43) (see transport model in Fig. 6*A*). Based on their biophysical and pharmacological properties and on their expression pattern, we have previously postulated that KCNQ1/KCNE3 channels fulfill this role (22). This postulate hinged largely on the specificity of chromanol 293B as an inhibitor of KCNQ1/KCNE3 channels. However, this drug may also inhibit other channels including CFTR (46), which needs ~6-fold larger concentrations for inhibition.

We now stringently tested this hypothesis by comparing short circuit currents (I_{sc}) across colonic epithelia from WT and *kcne3*$^{-/-}$ mice in Ussing chamber experiments (Fig. 6, *B*–*F*). To better isolate Cl^- currents, apical ENaC Na^+ channels were inhibited by 10 μM amiloride. The addition of 10 μM forskolin, which stimulates intracellular cAMP synthesis, led to a large and sustained increase in I_{sc} in WT colon (Fig. 6, *B* and *D*). This current component is carried by Cl^- ions that flow through apical cAMP-stimulated CFTR Cl^- channels (47). The current could be efficiently inhibited by 10 μM chromanol 293B. In contrast to WT, *kcne3*$^{-/-}$ colon almost lacked forsko-

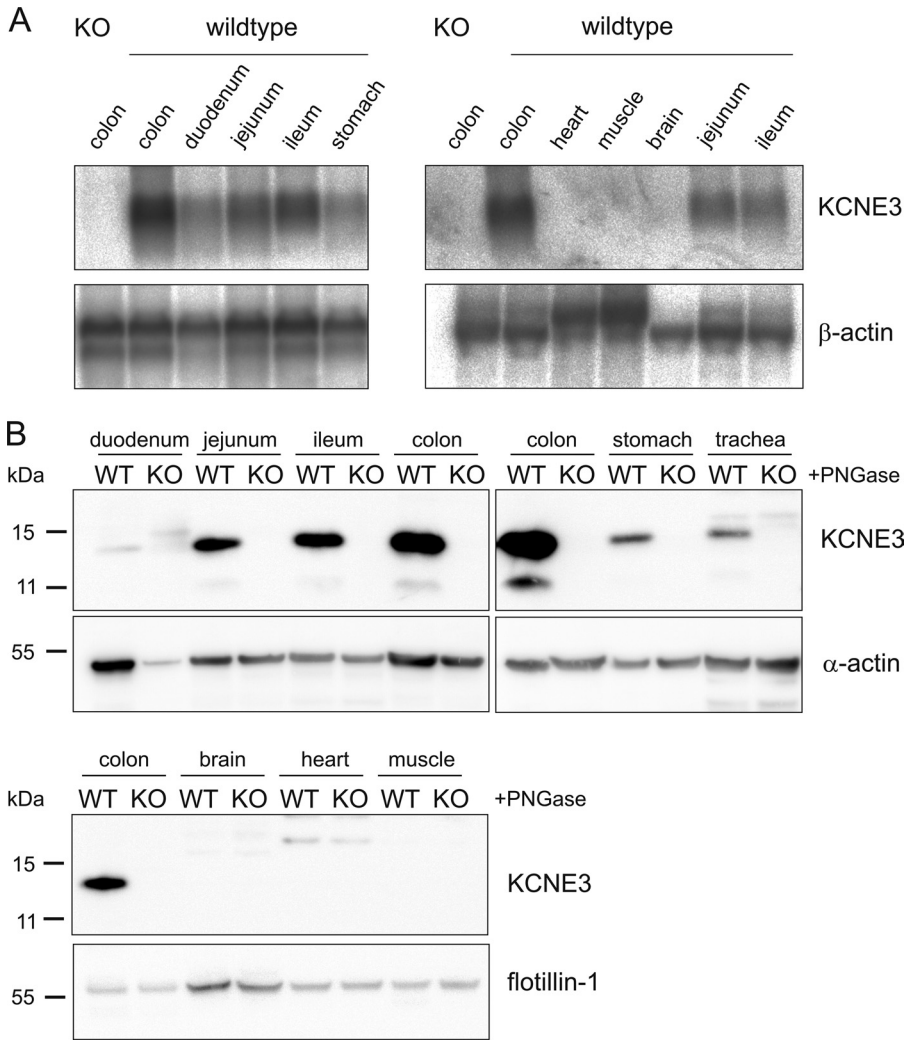

FIGURE 2. **Tissue distribution of KCNE3.** *A*, Northern blot analysis of *kcne3* expression. A *kcne3*-specific band was detected in WT mRNA from colon, duodenum, jejunum, ileum, and stomach but not in brain, heart, and skeletal muscle. Analysis of colonic mRNA from *kcne3*$^{-/-}$ (KO) mice proved specificity of the *kcne3* probe. Hybridization with a *β*-actin probe was used as loading control. *B*, Western blot analysis of KCNE3 expression in WT and *kcne3*$^{-/-}$ tissues. A single KCNE3-immunoreactive band (~14 kDa) was detected in deglycosylated membrane fractions from duodenum, jejunum, ileum, colon, stomach, and trachea from WT mice but not from KO mice. Deglycosylation proved necessary to obtain a specific, single band (see supplemental Fig. S2). No KCNE3 protein was detected in the brain, heart, and liver of WT mice. *α*-Actin and flotillin-1 served as loading controls.

lin-stimulated currents (Fig. 6, *C* and *D*). The application of chromanol 293B had no effect, agreeing with the absence of a chromanol 293B-sensitive component of whole cell currents from colonic crypt cells (supplemental "Results" and Fig. S5). The subsequent addition of 100 μM carbachol, which raises intracellular Ca^{2+} by stimulating muscarinic receptors, led to increases in I_{sc} that were on average indistinguishable between WT and KO tissues (Fig. 6*D*). Similar results were obtained with tissue samples taken from the proximal, middle, and distal parts of the colon (data not shown). Consistent with our finding that KCNQ1/KCNE3 channels are also expressed in the small intestine (Fig. 3, *A* and *C*), Ussing chamber experiments with jejunal and ileal epithelia revealed similar consequences of *kcne3* disruption (Fig. 6, *D* and *E*), although they appeared less pronounced. Whereas forskolin-induced currents were reduced by 70–80% in *kcne3*$^{-/-}$ colon, they were diminished by only 50–60% in jejunum and ileum in *kcne3*$^{-/-}$ mice. However, cholera toxin-stimulated fluid secretion into isolated small intestinal loops *in vivo* failed to reveal differences between WT and *kcne3*$^{-/-}$ mice (supplemental Fig. S4).

We conclude that a KCNE3-containing C293B-sensitive K^+ channel is crucial for cAMP-stimulated but not for Ca^{2+}-stimulated Cl^- secretion (48, 49) across intestinal epithelia. Consistent with its higher expression in colon, KCNE3 had a larger impact on colonic transport than on ileal or jejunal Cl^- transport. Its lack did not protect against cholera toxin-induced small intestinal fluid secretion.

KCNQ1/KCNE3 Channels in Tracheal Cl^- Secretion—Like colonic epithelium, airway epithelia are known to transport Cl^- and Na^+ in a CFTR- and ENaC-dependent manner. The disturbance of the airway surfaced liquid is a major factor in the pathology of cystic fibrosis. Because KCNE3 is expressed in the surface epithelia of the trachea (Fig. 5), we studied equivalent short circuit currents (I_{sc}) of tracheal preparations in Ussing chamber experiments (Fig. 7). Basal I_{sc} was not different between the genotypes (Fig. 7, *A* and *C*). Approximately half of this current was due to electrogenic Na^+ resorption as indicated by the effect of the ENaC inhibitor amiloride (20 μM) (Fig. 7, *A* and *C*). Differences between the amiloride-sensitive currents of WT and KO trachea were statistically not significant ($p = 0.2$).

I_{sc} was increased upon application of forskolin and IBMX, both of which raise intracellular cAMP without directly increasing Ca^{2+} (Fig. 7, *A* and *D*). The cAMP-stimulated, C293B-sensitive current component was almost absent in *kcne3*$^{-/-}$ mice (Fig. 7, *A* and *D*). In tracheal epithelium, purinergic receptor (P2Y) stimulation raises both intracellular Ca^{2+} and cAMP (50), thereby activating apical Ca^{2+}-activated and CFTR Cl^- channels, as well as basolateral KCNQ1/KCNE3 and Ca^{2+}-activated K^+ channels. Compared with forskolin/IBMX, apical ATP (100 μM) caused a larger increase in I_{sc}. With WT trachea, I_{sc} was increased ~4-fold at its peak and then declined to a plateau value that was approximately twice as large as control. This ATP effect was nearly abolished in *kcne3*$^{-/-}$ trachea (Fig. 7, *B* and *E*).

By hyperpolarizing the plasma membrane, KCNQ1/KCNE3 channels may not only increase Cl^- secretion but also Na^+

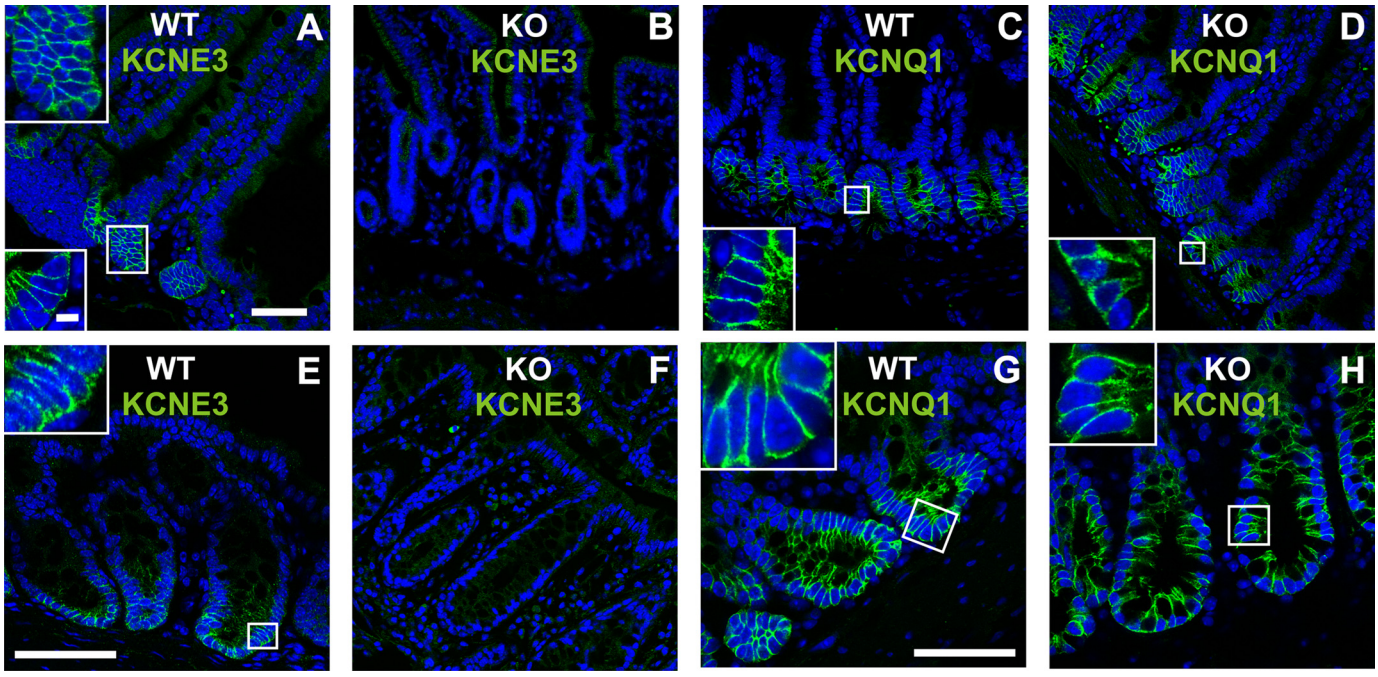

FIGURE 3. **Intestinal expression of KCNE3.** *A*, KCNE3 staining (*green*) was restricted to basolateral membranes of crypt cells of small intestine. *B*, lack of KCNE3 staining in *kcne3*$^{-/-}$ (KO) small intestine. *C* and *D*, staining for KCNQ1 (*green*) does not differ between WT (*C*) and *kcne3*$^{-/-}$ (*D*) small intestine. *E* and *F*, KCNE3 resides in basolateral membranes of colonic crypt cells (*E*) and is absent from KO colon (F). *G* and *H*, immunostaining for KCNQ1 (*green*) in WT colon (*G*) is similar to that in *kcne3*$^{-/-}$ colon (*H*). Counterstaining by Topro-3 (*blue*). The *insets* show higher magnifications of regions shown in frames, except for the *lower left inset* of *A* that is from a different section and highlights KCNE3 expression in basolateral membranes. The *inset scale bar* is 5 μm and applies for all insets. The *scale bar* in *A* applies also for *B–D*, the *scale bar* in *E* also applies for *F*, and the *scale bar* in *G* also applies for *H*. These *scale bars* represent 50 μm.

resorption. To isolate Cl^- currents, we performed experiments in the luminal presence of 20 μM amiloride (Fig. 7, *F* and *G*). Again, the response to forskolin/IBMX was drastically reduced in *kcne3*$^{-/-}$ trachea, suggesting a crucial role for KCNQ1/KCNE3 channels in cAMP-stimulated Cl^- secretion. The response to either ATP or carbachol was reduced to a lesser extent (by ~50%). It thus appears that Ca^{2+}-activated K^+ channels can substitute partially for KCNQ1/KCNE3 under these conditions.

Role of KCNE3 in Skeletal Muscle Function—Kv3.4/KCNE3 heteromeric K^+ channels have been suggested to set the resting membrane potential of skeletal muscle (28). A R83H sequence variant of KCNE3 was found in patients from two families with periodic paralysis, leading to the proposal that mutations in *KCNE3* underlie some forms of this genetically heterogeneous human disease (28, 30). However, we never observed spontaneous paralysis nor myotonia or abnormal movements in *kcne3*$^{-/-}$ mice. Histological analysis of skeletal muscle did not show morphological abnormalities (supplemental Fig. S1, *I–L*), contrasting with the vacuoles and tubular aggregates observed in muscle biopsies from some of the patients described to have KCNE3-related periodic paralysis (28). Because one of the patients reported by Abbot *et al.* (28) appeared to have hypokalemic periodic paralysis (in which the phenotype is precipitated by low K^+), we also put *kcne3*$^{-/-}$ mice and their WT littermates on a K^+-depleted diet for 2 weeks. Although this diet decreased serum K^+ levels from 6.5 to 3.5 mM in either genotype, no attacks of paralysis were observed. Rotarod tests did not reveal any differences between the genotypes under these circumstances, either. The time mice were able to stay on the turning and slowly accelerating rods was 4.02 ± 0.42 min (WT, $n = 8$) *versus* 4.24 ± 0.8 min (KO, $n = 8$) under normal diet and 4.23 ± 0.29 min (WT, $n = 8$) *versus* 4.36 ± 0.45 min (KO, $n = 8$) under K^+-depleted diet. Thus, the analysis of *kcne3*$^{-/-}$ mice does not support the notion that KCNE3 plays a crucial role in muscle physiology, a conclusion strongly bolstered by the lack of skeletal muscle expression of KCNE3 on both mRNA and protein levels (Fig. 2).

DISCUSSION

KCNE3, like other members of this gene family of K^+ channel β-subunits, shows rather promiscuous interactions with various pore-forming K^+ channel α-subunits when overexpressed heterologously. The present analysis of *kcne3*$^{-/-}$ mice demonstrates the importance of KCNQ1/KCNE3 for ion transport across intestinal and airway epithelia while questioning the postulated role of Kv3.4/KCNE3 heteromers in skeletal muscle physiology and pathology (28).

KCNE3 and Periodic Paralysis—KCNE3 has been reported to form heteromers with Kv3.4 in skeletal muscle and to significantly alter its biophysical properties (28, 51). A R83H sequence variant was described in affected members of two families with dominant periodic paralysis (28) and in one of fifteen patients with thyrotoxic hypokalemic periodic paralysis (30). WT KCNE3 increased, whereas KCNE3(R83H) decreased Kv3.4 peak currents in heterologous expression. Other experiments suggested that Kv3.4/KCNE3 largely sets the resting potential of cells and that the R83H mutant depolarizes Kv3.4-expressing cells in a dominant manner (28). However, subsequent reports showed that the R83H allele is also present in healthy controls (31, 32, 52) at a frequency of ~1% (52). This observation suggests that the R38H variant is rather a benign

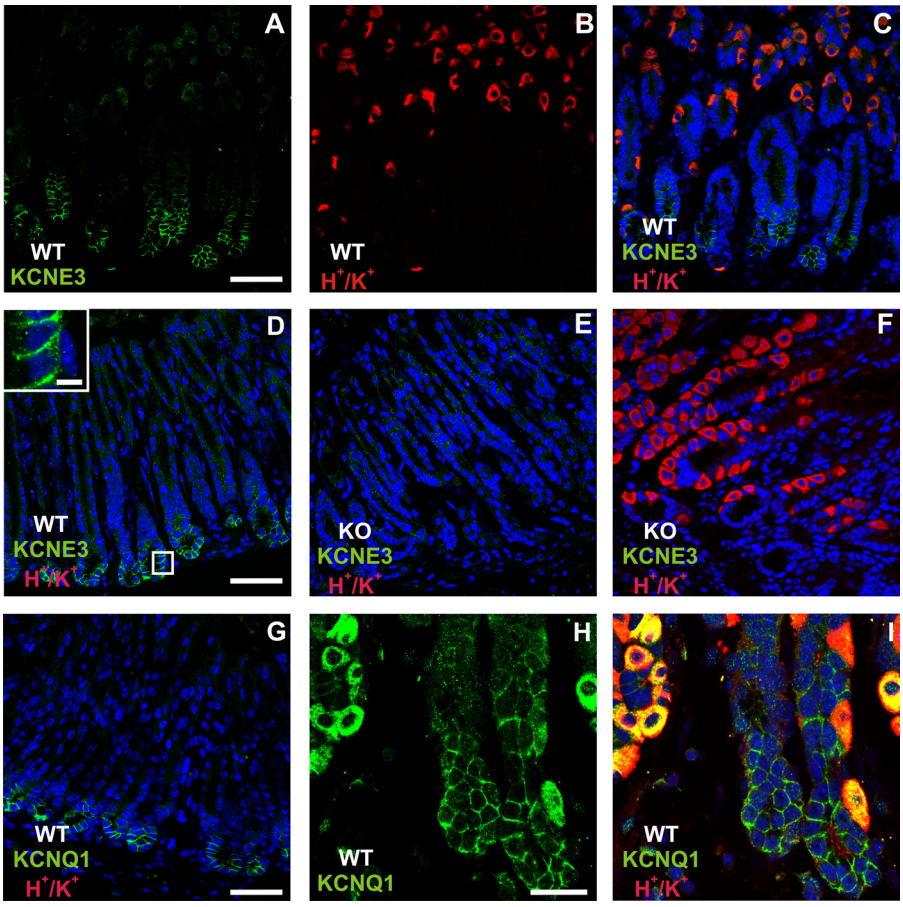

FIGURE 4. **Localization of KCNE3 in the stomach.** *A–D*, immunostaining for KCNE3 (*A*, *C*, and *D*; *green*) and H^+/K^+ ATPase (*B–D*; *red*) in gastric mucosa. KCNE3 is found in basolateral membranes of epithelial cells in the basal region of gastric glands that are devoid of the H^+/K^+ ATPase (*A*, *C*, and *D*). KCNE3 is expressed both in regions with a prominent presence of H^+/K^+ ATPase-expressing parietal cells (*A–C*) and in regions lacking those cells (*D*). *E* and *F*, KO controls for specificity of KCNE3 staining in areas lacking (*E*) or expressing (*F*) the H^+/K^+ ATPase. *G–I*, immunolocalization of KCNQ1 (*green*) and H^+/K^+ ATPase (*red*) in regions lacking (*G*) or expressing (*H* and *I*) the ATPase. KCNQ1 and the ATPase co-localize in parietal cells in a staining pattern broadly covering the cytoplasm. KCNQ1 is additionally present at the bottom of gastric glands in basolateral membranes of cells lacking H^+/K^+ ATPase (*G*). These cells express KCNE3 (*A–D*). KCNQ1 staining was similar in *kcne3*$^{-/-}$ stomach (data not shown). Counterstaining by Topro-3 (*blue*). The *inset scale bar* in *D*, which shows a higher magnification of the marked area, is 5 μm. The *lower right scale bar* in *D* represents 50 μm and also applies to *E* and *F*.

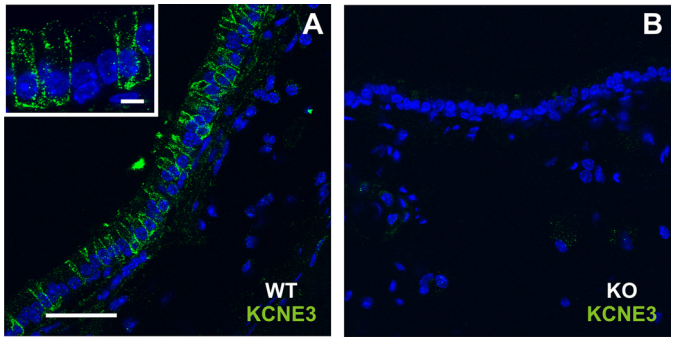

FIGURE 5. **Immunolocalization of KCNE3 in tracheal epithelium.** *A*, KCNE3 antibodies stain (in *green*) basolateral membranes of surface epithelial cells of WT (*A*) but not *kcne3*$^{-/-}$ trachea (*B*). *Inset*, higher magnification from a different tracheal section. Counterstaining by Topro-3 (*blue*). The *scale bar* is 25 μm, and the *inset scale bar* is 5 μm.

polymorphism. Whereas Abbott *et al.* (28) described robust KCNE3 expression in skeletal muscle, in our hands both mRNA and protein levels of KCNE3 were below the detection limit in skeletal muscle (Ref. 22 and the present work). When studied by quantitative reverse transcription-PCR, human skeletal muscle was almost devoid of *kcne3* mRNA (37). Together with the lack of a detectable skeletal muscle phenotype in *kcne3*$^{-/-}$ mice, these results argue against a role for KCNE3 in periodic paralysis.

KCNQ1/KCNE3 Channels in Transepithelial Transport—The present results very strongly support the hypothesis that KCNQ1/KCNE3 heteromers are involved in Cl^- secretion across intestinal and tracheal epithelia (22, 39). First evidence for a role of KCNQ1 came from the inhibition of colonic short circuit currents by chromanol 293B (40), a substance later shown to inhibit channels containing KCNQ1 subunits. C293B inhibits KCNQ1 homo-multimers with a K_i of roughly 27 μM, KCNQ1/KCNE1 heteromers with a K_i of ~7 μM, and KCNQ1/KCNE3 channels with a K_i of ~3 μM (22, 53).

Before KCNQ1/KCNE3 channels were identified (22), KCNQ1/KCNE1 heteromers were implicated in transport across colonic epithelia (54). However, expression levels of KCNE1 are low or even below detection limit in colon and trachea (39), and forskolin-stimulated intestinal Cl^- secretion was normal in *kcne1*$^{-/-}$ mice (55, 56). The co-localization of KCNQ1 and KCNE3 in basolateral membranes and the almost complete loss of C293B-inhibitable currents in *kcne3*$^{-/-}$ mice now very strongly support a crucial involvement of basolateral KCNQ1/KCNE3 heteromers in intestinal and tracheal Cl^- secretion.

Basolateral cAMP-activated K^+ channels were proposed to stimulate cAMP-dependent colonic Cl^- secretion by recycling K^+ for the basolateral NaK2Cl co-transporter NKCC1 and by hyperpolarizing the cell (22, 40, 41, 43). This hyperpolarization counteracts the depolarizing Cl^- efflux through CFTR and increases the electrochemical driving force for apical Cl^- secretion. This model (Fig. 6*A*) agrees with the co-expression of CFTR (57), NKCC1 (58, 59), and KCNQ1/KCNE3 in colonic crypts, the site of fluid and electrolyte secretion (60). In a minimal model, KCNQ1/KCNE3 would provide the only basolateral K^+ conductance, and CFTR would be the sole apical Cl^- channel. A rise in intracellular cAMP activates both CFTR and KCNQ1/KCNE3, leading to luminal Cl^- secretion. This model explains the inhibition of cAMP-stimulated electrogenic Cl^- secretion by C293B and its absence in *kcne3*$^{-/-}$ colon. How-

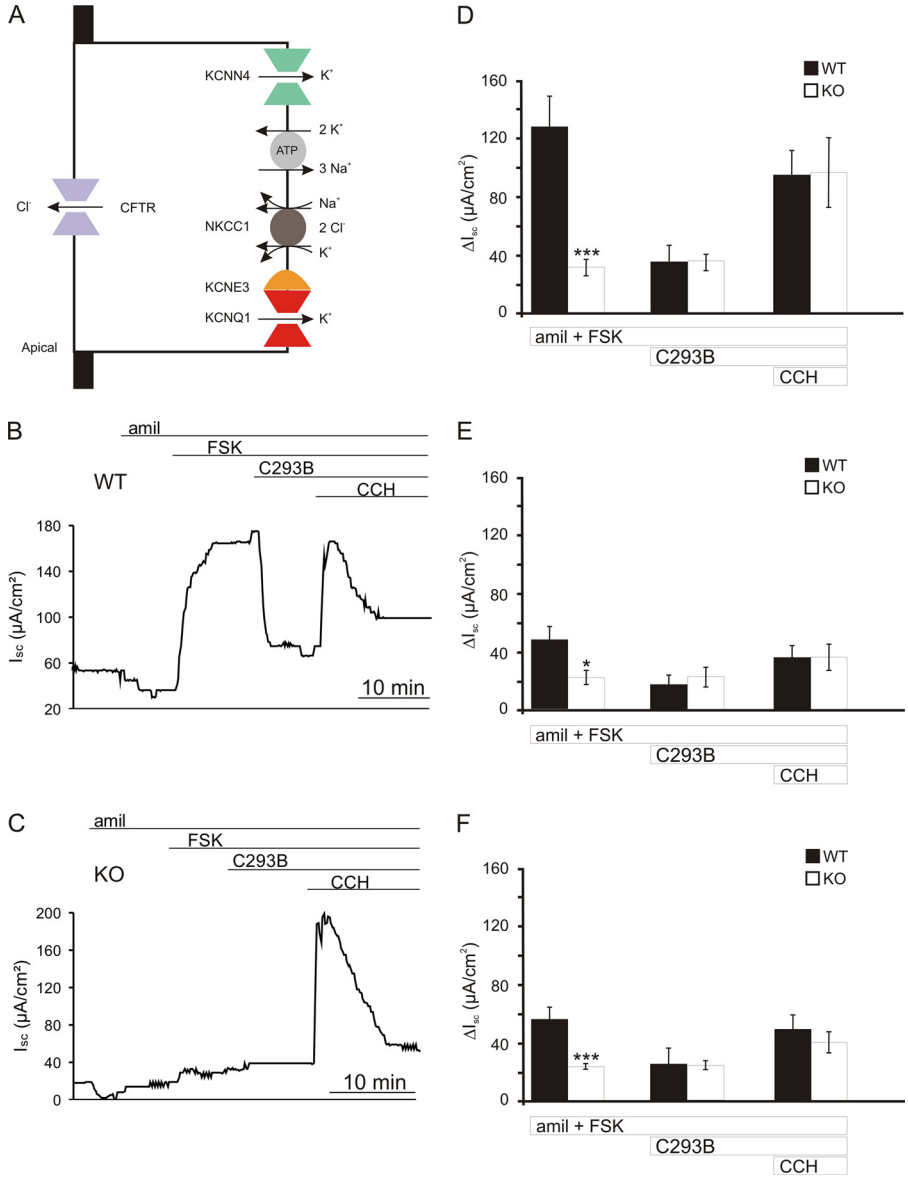

FIGURE 6. **Transepithelial transport across intestinal epithelia of WT and *kcne3*$^{-/-}$ mice.** *A*, cell model for intestinal Cl^- secretion by a colonic crypt cell. Driven by the Na^+ gradient established by the basolateral Na^+/K^+-ATPase, Na^+ powers the basolateral NaK2Cl co-transporter NKCC1, raising intracellular Cl^- above its electrochemical equilibrium. Hence Cl^- can exit the cell passively through apical, cAMP-stimulated CFTR Cl^- channels, resulting in Cl^- secretion. Basolateral K^+ channels are needed to recycle K^+. These channels additionally render the cell interior more negative, increasing the driving force for apical Cl^- exit. Colonic cells express both cAMP-activated KCNQ1/KCNE3 K^+ channels and Ca^{2+}-activated KCNN4 (SK4, $K_{Ca}3.1$) K^+ channels. The epithelial sodium channel ENaC, which we inhibited with amiloride in our experiments, is rather expressed in surface epithelial cells (63) and therefore not included in the cell model. *B* and *C*, representative traces from Ussing chamber experiments showing short circuit currents (I_{sc}) across WT (*B*) and *kcne3*$^{-/-}$ (*C*) distal colon clamped to 0 mV. Luminal amiloride (*amil*; 0 μM), serosal forskolin (*FSK*; 10 μM), serosal chromanol 293B (*C293B*; 10 μM), and serosal carbachol (*CCH*, 100 μM) were present as indicated by the *bars*. *D–F*, mean ΔI_{sc} from WT and KO distal colon (*D*), jejunum (*E*), and ileum (*F*) under different conditions (data from six or seven WT and six KO mice; means ± S.E.; ***, $p < 0.0001$ (colon) and $p < 0.0002$ (ileum); *, $p < 0.03$ (unpaired *t* test)). The resistance of the colonic tissues was 66.8 ± 5.2 (WT) and 68.4 ± 5.0 (KO) Ωcm^2, of jejunum 55.2 ± 6.6 (WT) and 56.0 ± 5.2 (KO), and of ileum 59.5 ± 3.5 (WT) and 49.7 ± 4.8 (KO) Ωcm^2. The resistance of the fluid amounted to 19–25 Ωcm^2.

ever, this picture is not complete, because carbachol increased I_{sc} in the presence of forskolin when KCNQ1/KCNE3 was either inhibited by C293B or absent in *kcne3*$^{-/-}$ colon (Fig. 6, *B–D*). Through activation of muscarinic receptors, carbachol increases intracellular Ca^{2+}. The ensuing activation of colonic basolateral Ca^{2+}-sensitive KCNN4 (SK4) K^+ channels (49, 61) can apparently fully compensate for the loss of KCNQ1/KCNE3 transport activity. Such a full compensation is not observed in trachea, where the KO of KCNE3 reduced ATP- or carbachol-stimulated I_{sc} by ~50% (Fig. 7). In trachea, there is an additional important contribution from apical Ca^{2+}-activated Cl^- channels (probably TMEM16A) (62) that operate in parallel to CFTR. These Ca^{2+}-activated channels may explain that carbachol increases I_{sc} across the trachea also in the absence of forskolin-induced increases in cAMP. KCNQ1/KCNE3 channels, which have basal activity also without cAMP stimulation (22), contribute to the driving force for apical Cl^- exit through both types of Cl^- channels.

In cells expressing apical ENaC channels, KCNQ1/KCNE3-mediated hyperpolarization should also increase Na^+ absorption. This may occur in trachea, but not in the distal colon, where ENaC may only be expressed in surface epithelial cells (63), but not in crypts, the predominant site of KCNQ1/KCNE3 expression. Therefore, KCNE3 is not expected to have a major influence on aldosterone-induced colonic Na^+ absorption.

The quantitative contribution of specific basolateral K^+ channels to the secretory response differs between colon and small intestine, with KCNE3 being more important in colon than in jejunum or ileum. The rather moderate dependence of small intestinal cAMP-dependent Cl^- secretion on KCNE3 (~45% of current remaining in *kcne3*$^{-/-}$ jejunum or ileum) agrees quantitatively very well with the degree of inhibition of cAMP-stimulated jejunal Cl^- secretion in *kcnq1*$^{-/-}$ mice (64). This comparison provides strong support for a crucial role of KCNQ1/KCNE3 heteromeric channels, which cannot be replaced functionally by KCNQ1 homo-oligomers. The cAMP-dependent currents remaining in *kcne3*$^{-/-}$ small intestine may explain, at least in part, our observation that cholera toxin-stimulated *in vivo* fluid secretion did not differ between WT and *kcne3*$^{-/-}$ ileum (supplemental Fig. S4). Others have shown in similar experiments that cholera toxin-stimulated small intestinal fluid secretion can be blocked by CFTR inhibitors

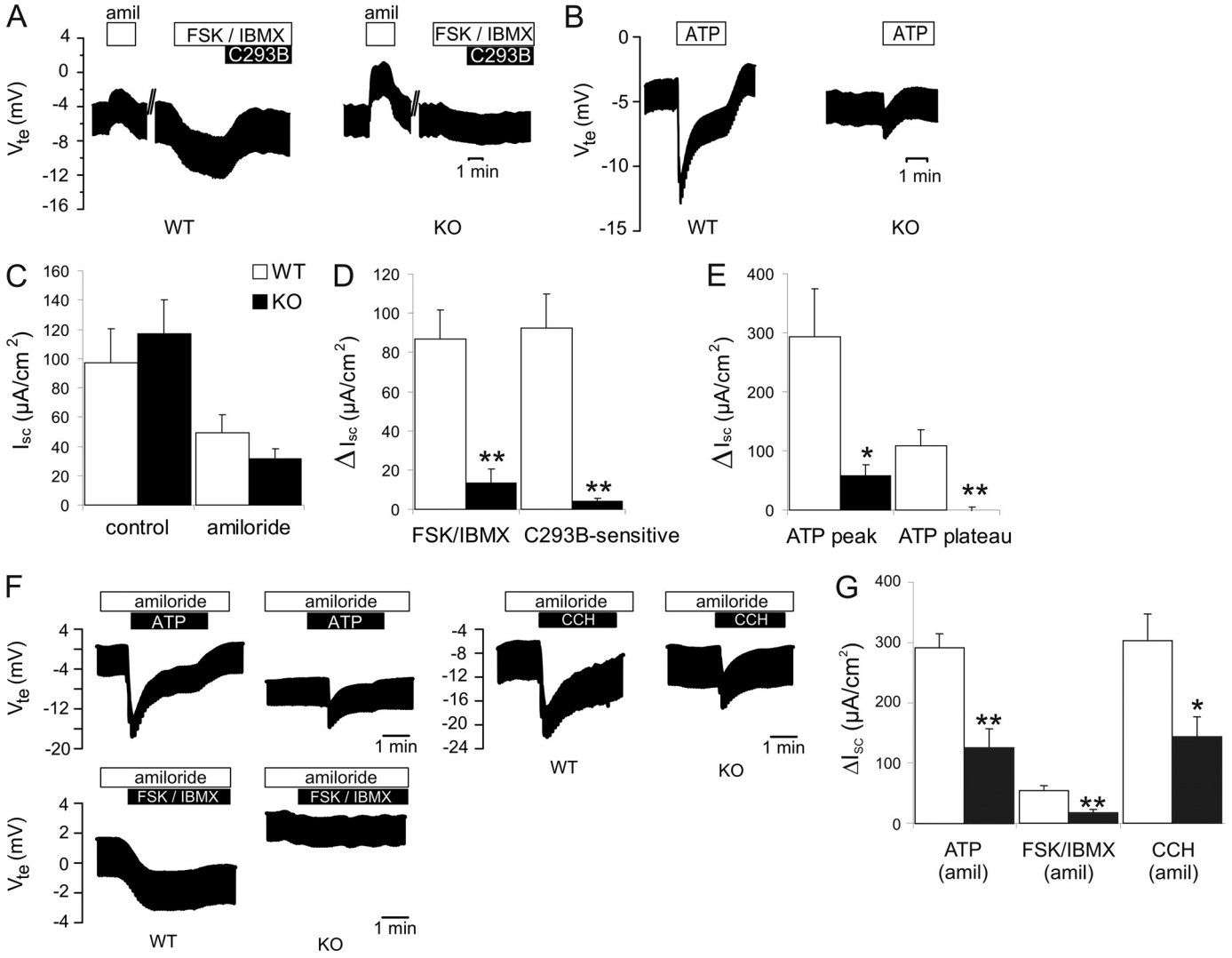

FIGURE 7. **Effect of secretagogues on ion transport by tracheal epithelia from WT and *kcne3*$^{-/-}$ mice measured under current-clamp conditions.** *A*, Ussing-chamber recording of transepithelial voltage (V_{te}) across WT (*left panel*) and KO (*right panel*) tracheal samples. The *upper border* of the *line* shows V_{te}, and the length of the downward voltage deflections reflects the transepithelial resistance (R_{te}). Luminal application of amiloride (20 μM), and basolateral FSK (2 μM), IBMX (100 μM), and C293B (10 μM) is indicated above. *B*, similar recordings exploring effects of luminal ATP (100 μM). ATP caused a rapid transient increase ("peak") of V_{te} in WT trachea, followed by a steady state lumen-negative V_{te}. Both deflections were drastically reduced in the KO. *C*, mean calculated short circuit current (I_{sc}) before and after application of amiloride (10 μM) (number of measurements: WT, twelve; KO, eleven; one/animal). *D*, differential currents (ΔI_{sc}) induced by 2 μM forskolin (FSK) and 100 μM IBMX (*left bars*) and calculated C293B-sensitive component of forskolin-stimulated current (*right bars*). *E*, maximal (peak) and steady state (plateau) differential currents ΔI_{sc} induced by 100 μM ATP (values averaged from twelve (WT) and ten (KO) experiments (one/mouse). *F* and *G*, similar experiments in the presence of 20 μM amiloride to abolish Na^+-transport. *F*, original recordings showing effects of luminal ATP (100 μM), FSK (2 μM) + IBMX (100 μM), and carbachol (100 μM) on WT and KO tracheas. *G*, mean differential currents (ΔI_{sc}) induced by 100 μM ATP, 2 μM FSK + 100 μM IBMX, or 100 μM carbachol, always in the presence of 20 μM amiloride. Number of measurements (animals): WT, seven; KO, seven. *, $p < 0.05$; **, $p < 0.005$. The resistance values of the tracheal tissue samples were 42.2 ± 2.6 (WT; $n = 12$) and 46.1 ± 2.6 (KO; $n = 12$) Ωcm^2. The resistance of the fluid in the Ussing chamber was 3.4 ± 2.1 Ωcm^2.

(65) or by clotrimazole (66). The latter inhibitor acts on both KCNQ1/KCNE3 (22) and Ca^{2+}-activated K^+ channels like KCNN4 (SK4) (49). Taken together, these results suggest a more important role for basolateral Ca^{2+}-activated K^+ channels in small intestinal Cl^- and fluid secretion and cross-talk between cAMP and Ca^{2+} signaling in that tissue. Such cross-talk may be particularly relevant for our *in vivo* experiments, because under these conditions cholera toxin may stimulate intestinal secretion not only by direct effects on epithelial cells but also through activation of the enteric nervous system and release of several mediators that may act on the $[Ca^{2+}]_i$ of mucosal cells (67).

In stomach, KCNE3 was detected in basolateral membranes of epithelial cells at the bottom of gastric glands, but not in acid-secreting parietal cells. These latter cells express KCNQ1/KCNE2 channels in tubulovesicular and apical membranes (19, 29). By recycling K^+ for the gastric H^+/K^+ ATPase, these channels are crucial for gastric acid secretion, as revealed by disruption of either *kcnq1* (16, 64) or *kcne2* (19) in mice. Whereas both of these mouse models had gastric gland hyperplasia (16, 19), no morphological abnormalities were detectable in *kcne3*$^{-/-}$ stomach (supplemental Fig. S1, *A* and *B*). Our results thus indicate that KCNQ1/KCNE3 plays no role in gastric acid secretion. Its localization in basolateral membranes at the bottom of glands rather suggests a role in salt and fluid secretion as in intestine and trachea. Such fluid secretion may be needed to flush the digestive enzymes exocytosed by those cells, or the acid secreted by parietal cells, into the lumen of the stomach.

The normal expression of KCNQ1 in *kcne3*$^{-/-}$ intestine implies that KCNE3 is necessary neither for the localization nor the stability of the KCNQ1 α-subunit. This contrasts, for instance, with the results for CLC Cl^- transport proteins, where the loss of β-subunits drastically decreased the abundance of their cognate α-subunits (68, 69). Our results agree with the observation that KCNQ1 traffics to the plasma membrane of transfected cell also without KCNE3, but KCNE3 needs KCNQ1 to reach that location (22). Whereas KCNQ1 homomultimers and KCNQ1/KCNE3 heteromers reside in basolateral membranes, heteromers formed of KCNQ1 with either KCNE1 (70) or KCNE2 (18) localize to the apical plasma membrane, suggesting a role for those β-subunits in targeting.

KCNQ1 is physiologically nonfunctional without KCNE3 in the intestine and trachea, although the abundance and localization of the ion-conducting α-subunit are not changed. Whereas KCNQ1/KCNE1 heteromers can efficiently transport K^+ ions across the very depolarized (+5 mV) apical membrane of marginal cells of the stria vascularis (10), their voltage dependence (20, 21) predicts that they will be largely closed at the negative voltages present across the basolateral membranes of colonic (41) or tracheal (71) epithelial cells (−60 and −35 mV, respectively). The nearly voltage-independent conductance of KCNQ1/KCNE3 heteromers, in contrast, fits perfectly to a role in transepithelial transport (22). Moreover, whereas KCNQ1 and KCNQ1/KCNE3 channels mediate currents of similar magnitude at positive voltages when expressed in *Xenopus* oocytes (22), KCNQ1 currents were enhanced more than 3-fold by KCNE3 in COS (23) or Chinese hamster ovary cells (72). The drastic reduction in transepithelial transport in *kcne3*$^{-/-}$ mice, together with the normal abundance and localization of KCNQ1, directly demonstrates that the change of KCNQ1 transport properties by KCNE3 is essential for its physiological role.

Taking into account previous work on KCNE1 (7–11) and KCNE2 (15, 19), it appears that KCNQ1 always needs a KCNE β-subunit for proper physiological function. The present analysis of *kcne3*$^{-/-}$ mice, which does not hinge on the specificity of K^+ channel inhibitors, strongly supports an important role for KCNQ1/KCNE3 channels in salt and fluid secretion across intestinal and tracheal epithelia while questioning the purported role of Kv3.4/KCNE3 K^+ channels in human periodic paralysis (28). Although KCNQ1/KCNE3 plays a crucial role in driving colonic Cl^- secretion, it is not essential for fluid secretion in the small intestine. Hence KCNQ1/KCNE3 inhibitors will be of limited use in cholera or other severe forms of diarrhea. The critical importance of KCNE3 for tracheal transport suggests *KCNE3* as a modifier gene in cystic fibrosis.

Acknowledgments—We thank I. Lauterbach for technical assistance, Dr. I. Hermans-Borgmeyer for help with the transgenic mouse generation, and Dr. M. Beyermann for peptide synthesis.

REFERENCES

1. Scott, V. E., Rettig, J., Parcej, D. N., Keen, J. N., Findlay, J. B., Pongs, O., and Dolly, J. O. (1994) *Proc. Natl. Acad. Sci. U.S.A.* **91,** 1637–1641
2. Takumi, T., Ohkubo, H., and Nakanishi, S. (1988) *Science* **242,** 1042–1045
3. Aguilar-Bryan, L., Nichols, C. G., Wechsler, S. W., Clement, J. P., Boyd, A. E., 3rd, González, G., Herrera-Sosa, H., Nguy, K., Bryan, J., and Nelson, D. A. (1995) *Science* **268,** 423–426
4. Sanguinetti, M. C. (2000) *Trends Pharmacol. Sci.* **21,** 199–201
5. McCrossan, Z. A., and Abbott, G. W. (2004) *Neuropharmacology* **47,** 787–821
6. Abbott, G. W., Sesti, F., Splawski, I., Buck, M. E., Lehmann, M. H., Timothy, K. W., Keating, M. T., and Goldstein, S. A. (1999) *Cell* **97,** 175–187
7. Tyson, J., Tranebjaerg, L., Bellman, S., Wren, C., Taylor, J. F., Bathen, J., Aslaksen, B., Sorland, S. J., Lund, O., Malcolm, S., Pembrey, M., Bhattacharya, S., and Bitner-Glindzicz, M. (1997) *Hum. Mol. Genet* **6,** 2179–2185
8. Splawski, I., Tristani-Firouzi, M., Lehmann, M. H., Sanguinetti, M. C., and Keating, M. T. (1997) *Nat. Genet.* **17,** 338–340
9. Schulze-Bahr, E., Wang, Q., Wedekind, H., Haverkamp, W., Chen, Q., Sun, Y., Rubie, C., Hordt, M., Towbin, J. A., Borggrefe, M., Assmann, G., Qu, X., Somberg, J. C., Breithardt, G., Oberti, C., and Funke, H. (1997) *Nat. Genet.* **17,** 267–268
10. Vetter, D. E., Mann, J. R., Wangemann, P., Liu, J., McLaughlin, K. J., Lesage, F., Marcus, D. C., Lazdunski, M., Heinemann, S. F., and Barhanin, J. (1996) *Neuron* **17,** 1251–1264
11. Drici, M. D., Arrighi, I., Chouabe, C., Mann, J. R., Lazdunski, M., Romey, G., and Barhanin, J. (1998) *Circ. Res.* **83,** 95–102
12. Tinel, N., Diochot, S., Borsotto, M., Lazdunski, M., and Barhanin, J. (2000) *EMBO J.* **19,** 6326–6330
13. Tinel, N., Diochot, S., Lauritzen, I., Barhanin, J., Lazdunski, M., and Borsotto, M. (2000) *FEBS Lett.* **480,** 137–141
14. Zhang, M., Jiang, M., and Tseng, G. N. (2001) *Circ. Res.* **88,** 1012–1019
15. Roepke, T. K., Kontogeorgis, A., Ovanez, C., Xu, X., Young, J. B., Purtell, K., Goldstein, P. A., Christini, D. J., Peters, N. S., Akar, F. G., Gutstein, D. E., Lerner, D. J., and Abbott, G. W. (2008) *FASEB J.* **22,** 3648–3660
16. Lee, M. P., Ravenel, J. D., Hu, R. J., Lustig, L. R., Tomaselli, G., Berger, R. D., Brandenburg, S. A., Litzi, T. J., Bunton, T. E., Limb, C., Francis, H., Gorelikow, M., Gu, H., Washington, K., Argani, P., Goldenring, J. R., Coffey, R. J., and Feinberg, A. P. (2000) *J. Clin. Invest.* **106,** 1447–1455
17. Grahammer, F., Herling, A. W., Lang, H. J., Schmitt-Graff, A., Wittekindt, O. H., Nitschke, R., Bleich, M., Barhanin, J., and Warth, R. (2001) *Gastroenterology* **120,** 1363–1371
18. Heitzmann, D., Grahammer, F., von Hahn, T., Schmitt-Graff, A., Romeo, E., Nitschke, R., Gerlach, U., Lang, H. J., Verrey, F., Barhanin, J., and Warth, R. (2004) *J. Physiol.* **561,** 547–557
19. Roepke, T. K., Anantharam, A., Kirchhoff, P., Busque, S. M., Young, J. B., Geibel, J. P., Lerner, D. J., and Abbott, G. W. (2006) *J. Biol. Chem.* **281,** 23740–23747
20. Barhanin, J., Lesage, F., Guillemare, E., Fink, M., Lazdunski, M., and Romey, G. (1996) *Nature* **384,** 78–80
21. Sanguinetti, M. C., Curran, M. E., Zou, A., Shen, J., Spector, P. S., Atkinson, D. L., and Keating, M. T. (1996) *Nature* **384,** 80–83
22. Schroeder, B. C., Waldegger, S., Fehr, S., Bleich, M., Warth, R., Greger, R., and Jentsch, T. J. (2000) *Nature* **403,** 196–199
23. Bendahhou, S., Marionneau, C., Haurogne, K., Larroque, M. M., Derand, R., Szuts, V., Escande, D., Demolombe, S., and Barhanin, J. (2005) *Cardiovasc. Res.* **67,** 529–538
24. Nakajo, K., and Kubo, Y. (2007) *J. Gen. Physiol.* **130,** 269–281
25. MacVinish, L. J., Guo, Y., Dixon, A. K., Murrell-Lagnado, R. D., and Cuthbert, A. W. (2001) *Mol. Pharmacol.* **60,** 753–760
26. Lewis, A., McCrossan, Z. A., and Abbott, G. W. (2004) *J. Biol. Chem.* **279,** 7884–7892
27. McCrossan, Z. A., Lewis, A., Panaghie, G., Jordan, P. N., Christini, D. J., Lerner, D. J., and Abbott, G. W. (2003) *J. Neurosci.* **23,** 8077–8091
28. Abbott, G. W., Butler, M. H., Bendahhou, S., Dalakas, M. C., Ptacek, L. J., and Goldstein, S. A. (2001) *Cell* **104,** 217–231
29. Dedek, K., and Waldegger, S. (2001) *Pflügers Arch.* **442,** 896–902
30. Dias Da Silva, M. R., Cerutti, J. M., Arnaldi, L. A., and Maciel, R. M. (2002) *J. Clin Endocrinol. Metab* **87,** 4881–4884
31. Sternberg, D., Tabti, N., Fournier, E., Hainque, B., and Fontaine, B. (2003) *Neurology* **61,** 857–859
32. Jurkat-Rott, K., and Lehmann-Horn, F. (2004) *Neurology* **62,** 1012–1015
33. Fontaine, B. (2009) *Adv. Genetics* **63,** 3–23
34. Günzel, D., Florian, P., Richter, J. F., Troeger, H., Schulzke, J. D., Fromm,

M., and Gitter, A. H. (2006) *Am. J. Physiol. Cell Physiol.* **290,** R1496–R1507
35. Stockmann, M., Gitter, A. H., Sorgenfrei, D., Fromm, M., and Schulzke, J. D. (1999) *Pflügers Arch.* **438,** 107–112
36. Gitter, A. H., Schulzke, J. D., Sorgenfrei, D., and Fromm, M. (1997) *J. Biochem. Biophys. Methods* **35,** 81–88
37. Lundquist, A. L., Turner, C. L., Ballester, L. Y., and George, A. L., Jr. (2006) *Genomics* **87,** 119–128
38. Liao, T., Wang, L., Halm, S. T., Lu, L., Fyffe, R. E., and Halm, D. R. (2005) *Am. J. Physiol.* **289,** C564–C575
39. Grahammer, F., Warth, R., Barhanin, J., Bleich, M., and Hug, M. J. (2001) *J. Biol. Chem.* **276,** 42268–42275
40. Lohrmann, E., Burhoff, I., Nitschke, R. B., Lang, H. J., Mania, D., Englert, H. C., Hropot, M., Warth, R., Rohm, W., Bleich, M., *et al.* (1995) *Pflügers Arch.* **429,** 517–530
41. Diener, M., Hug, F., Strabel, D., and Scharrer, E. (1996) *Br. J. Pharmacol.* **118,** 1477–1487
42. Warth, R., Riedemann, N., Bleich, M., Van Driessche, W., Busch, A. E., and Greger, R. (1996) *Pflügers Arch.* **432,** 81–88
43. Greger, R., Bleich, M., Riedemann, N., van Driessche, W., Ecke, D., and Warth, R. (1997) *Comp Biochem. Physiol. A Physiol.* **118,** 271–275
44. MacVinish, L. J., Hickman, M. E., Mufti, D. A., Durrington, H. J., and Cuthbert, A. W. (1998) *J. Physiol. (Lond)* **510,** 237–247
45. Zdebik, A. A., Cuffe, J. E., Bertog, M., Korbmacher, C., and Jentsch, T. J. (2004) *J. Biol. Chem.* **279,** 22276–22283
46. Bachmann, A., Quast, U., and Russ, U. (2001) *Naunyn Schmiedebergs Arch. Pharmacol.* **363,** 590–596
47. Clarke, L. L., Grubb, B. R., Gabriel, S. E., Smithies, O., Koller, B. H., and Boucher, R. C. (1992) *Science* **257,** 1125–1128
48. Strabel, D., and Diener, M. (1995) *Eur. J. Pharmacol.* **274,** 181–191
49. Warth, R., Hamm, K., Bleich, M., Kunzelmann, K., von Hahn, T., Schreiber, R., Ullrich, E., Mengel, M., Trautmann, N., Kindle, P., Schwab, A., and Greger, R. (1999) *Pflügers Arch.* **438,** 437–444
50. Köttgen, M., Löffler, T., Jacobi, C., Nitschke, R., Pavenstadt, H., Schreiber, R., Frische, S., Nielsen, S., and Leipziger, J. (2003) *J. Clin. Invest.* **111,** 371–379
51. Abbott, G. W., Butler, M. H., and Goldstein, S. A. (2006) *Faseb J.* **20,** 293–301
52. Jurkat-Rott, K., and Lehmann-Horn, F. (2007) *Neurotherapeutics* **4,** 216–224
53. Lerche, C., Bruhova, I., Lerche, H., Steinmeyer, K., Wei, A. D., Strutz-Seebohm, N., Lang, F., Busch, A. E., Zhorov, B. S., and Seebohm, G. (2007) *Mol. Pharmacol.* **71,** 1503–1511
54. Suessbrich, H., Bleich, M., Ecke, D., Rizzo, M., Waldegger, S., Lang, F., Szabo, I., Lang, H. J., Kunzelmann, K., Greger, R., and Busch, A. E. (1996) *FEBS Lett.* **396,** 271–275
55. Arrighi, I., Bloch-Faure, M., Grahammer, F., Bleich, M., Warth, R., Mengual, R., Drici, M. D., Barhanin, J., and Meneton, P. (2001) *Proc. Natl. Acad. Sci. U.S.A.* **98,** 8792–8797
56. Warth, R., García Alzamora, M., Kim, J. K., Zdebik, A., Nitschke, R., Bleich, M., Gerlach, U., Barhanin, J., and Kim, S. J. (2002) *Pflügers Arch.* **443,** 822–828
57. Strong, T. V., Boehm, K., and Collins, F. S. (1994) *J. Clin. Invest.* **93,** 347–354
58. Matthews, J. B., Hassan, I., Meng, S., Archer, S. Y., Hrnjez, B. J., and Hodin, R. A. (1998) *J. Clin. Invest.* **101,** 2072–2079
59. Reynolds, A., Parris, A., Evans, L. A., Lindqvist, S., Sharp, P., Lewis, M., Tighe, R., and Williams, M. R. (2007) *J. Physiol.* **582,** 507–524
60. Welsh, M. J., Smith, P. L., Fromm, M., and Frizzell, R. A. (1982) *Science* **218,** 1219–1221
61. Flores, C. A., Melvin, J. E., Figueroa, C. D., and Sepúlveda, F. V. (2007) *J. Physiol.* **583,** 705–717
62. Rock, J. R., O'Neal, W. K., Gabriel, S. E., Randell, S. H., Harfe, B. D., Boucher, R. C., and Grubb, B. R. (2009) *J. Biol. Chem.* **284,** 14875–14880
63. Amasheh, S., Milatz, S., Krug, S. M., Bergs, M., Amasheh, M., Schulzke, J. D., and Fromm, M. (2009) *Biochem. Biophys. Res. Commun.* **378,** 45–50
64. Vallon, V., Grahammer, F., Völkl, H., Sandu, C. D., Richter, K., Rexhepaj, R., Gerlach, U., Rong, Q., Pfeifer, K., and Lang, F. (2005) *Proc. Natl. Acad. Sci. U.S.A.* **102,** 17864–17869
65. Ma, T., Thiagarajah, J. R., Yang, H., Sonawane, N. D., Folli, C., Galietta, L. J., and Verkman, A. S. (2002) *J. Clin. Invest.* **110,** 1651–1658
66. Rufo, P. A., Merlin, D., Riegler, M., Ferguson-Maltzman, M. H., Dickinson, B. L., Brugnara, C., Alper, S. L., and Lencer, W. I. (1997) *J. Clin. Invest.* **100,** 3111–3120
67. Farthing, M. J., Casburn-Jones, A., and Banks, M. R. (2004) *Curr. Gastroenterol Rep.* **6,** 177–180
68. Lange, P. F., Wartosch, L., Jentsch, T. J., and Fuhrmann, J. C. (2006) *Nature* **440,** 220–223
69. Rickheit, G., Maier, H., Strenzke, N., Andreescu, C. E., De Zeeuw, C. I., Muenscher, A., Zdebik, A. A., and Jentsch, T. J. (2008) *EMBO J.* **27,** 2907–2917
70. Sugimoto, T., Tanabe, Y., Shigemoto, R., Iwai, M., Takumi, T., Ohkubo, H., and Nakanishi, S. (1990) *J. Membr. Biol.* **113,** 39–47
71. Kunzelmann, K., Kathofer, S., and Greger, R. (1995) *Pflügers Arch.* **431,** 1–9
72. Ohno, S., Toyoda, F., Zankov, D. P., Yoshida, H., Makiyama, T., Tsuji, K., Honda, T., Obayashi, K., Ueyama, H., Shimizu, W., Miyamoto, Y., Kamakura, S., Matsuura, H., Kita, T., and Horie, M. (2009) *Hum. Mutat.* **30,** 557–563